次世代観測装置用の新しい回折格子の開発状況

海老塚 昇[1], 岡本 隆之[1], 細畠 拓也[1], 山形 豊[1], 佐々木 実[2], 魚本 幸[3], 島津 武仁[3],
佐藤 慎也[4], 橋本 信幸[4], 田中 壱[5], 服部 暁[5], 尾崎 忍夫[5], 青木 和光[5]
1 理研, 2 豊田工大・工, 3 東北大・工, 4 シチズンHD・開発部, 5 国立天文台

Limitation of surface relief (SR) grating

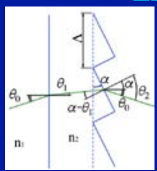

$$\sin\theta_0 = n\sin\theta_1$$
$$n\sin(\alpha-\theta_1) = \sin\theta_2$$
$$\theta_2 = \alpha+\theta_0$$
$$n\sin(\alpha-\theta_1) = \sin(\alpha+\theta_0)$$
$$n(\sin\alpha\cos\theta_1 - \sin\theta_1\cos\alpha) = \sin\alpha\cos\theta_0 + \sin\theta_0\cos\alpha$$
$$(n\cos\theta_1 - \cos\theta_0)\sin\alpha = (\sin\theta_0 + n\sin\theta_1)\cos\alpha = 2\sin\theta_0\cos\alpha$$
$$\tan\alpha = 2\sin\theta_0/(n\cos\theta_1 - \cos\theta_0)$$

n = 1.5, $\theta_0 \le 30°$ ($\theta_2 > 90°$)
n = 1.8, $\theta_0 \le 36°$
n = 2.3, $\theta_0 \le 45°$
n = 3.0, $\theta_0 \le 54°$
Diamond: n = 2.46@400nm

SR grating with saw tooth grooves is not feasible for the high-dispersion transmission grating.

Reflector facet transmission (RFT) grating

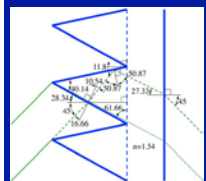

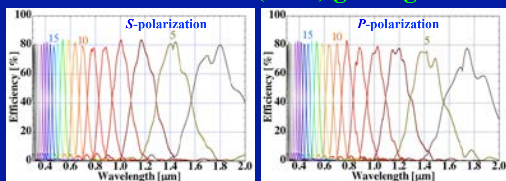

Diffraction efficiency calculated by RCWA. Λ=5μm, θ_0=45°, n_1=1.0, n_2=1.54

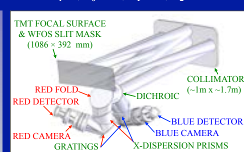

WFOS: Wide Field Optical Spectrograph.
The first generation instrument for TMT.
R~5000, ~10.000@0.75” slit

RTF gratings for WFOS	
Vertex angle	: γ = 35~45°
Period	: Λ= 2~5 μm
Size	: 400 x 550~750 [mm]

Hybrid grism for MOIRCS

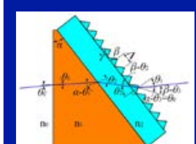

Prism material	: ZnSe (n_1= 2.4529@1.65 μm)
Plate	: S-FPM3 (n_2= 1.5240@1.65 μm)
Prism vertex angle	: α = 23.8°
Grating period	: Λ= 10.79μm (92.68 grooves/mm)
Incident angle	: θ_0= 5°
Groove blaze angle	: β = 64.8°
Groove vertex angle	: γ = 61.8°

Slit width: 0.3”
7th, R= 2,900@0.88 μm
6th, R= 2,790@1.02 μm
5th, R= 2,750@1.25 μm
4th, R= 2,800@1.65 μm
3rd, R= 2,770@2.20 μm

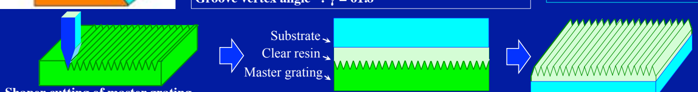

Shaper cutting of master grating.
Work: Ni-P alloy of non-electrolytic plating

Replication

Finish

Fabrication method of SR grating for RFT grating and MOIRCS hybrid grism

Ultra-high precision machine (Nagase-I, NPIC-M200).

Single-crystal diamond tool.

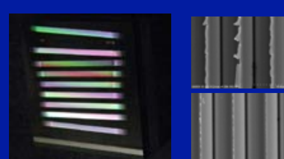

Test cuttings for condition setting.

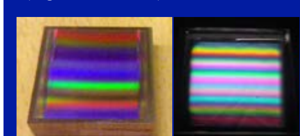

Mold for replication experiment (left), replica of mold (right). Work piece size: 50×50 [mm].

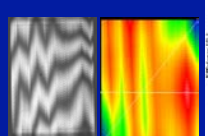

Wave front of mold.
P-V:0.89λ, RMS: 0.13λ.

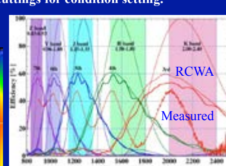

Diffraction efficiency of replicated transmission grating.

Echelle grism for MOIRCS

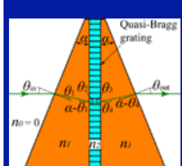

Schematic representation of echelle grism for MOIRCS

Slit width: 0.3”
5th, R= 4,630@1.02 μm
4th, R= 4,420@1.25 μm
3rd, R= 4,270@1.65 μm

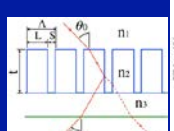

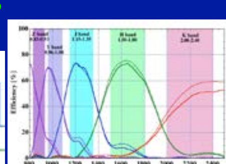

Schematic representation of volume binary grating (left) function as a quasi-Bragg (QB) grating and diffraction efficiency calculated by RCWA (right). L&S=4.6:0.5 [μm], θ_0=28.4°, n_1=1.33, n_2=1.6, n_3=1.6, t = 16 μm

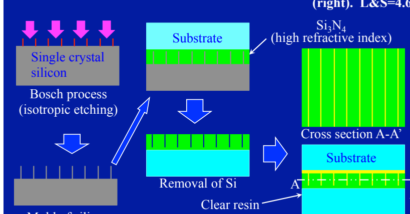

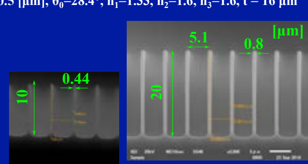

Silicon mold for volume binary grating. Fabricated by Nanotechnology platform of Toyota Institute of Technology.

Fabrication process of the volume binary grating

Birefringence volume phase holographic (B-VPH) grating

$$\eta_S = \sin^2\left\{\frac{\pi(n_{S\max}-n_{S\min})t}{\Lambda(n_{S\max}+n_{S\min})\sin 2\theta_S}\right\} \quad \eta_P = \sin^2\left\{\frac{\pi(n_{P\max}-n_{P\min})t\cos 2\theta_P}{\Lambda(n_{P\max}+n_{P\min})\sin 2\theta_P}\right\}$$

$$\frac{(n_{S\max}-n_{S\min})}{(n_{S\max}+n_{S\min})\sin 2\theta_S} = \frac{(n_{P\max}-n_{P\min})\cos 2\theta_P}{(n_{P\max}+n_{P\min})\sin 2\theta_P}$$

$$\frac{(n_{S\max}-n_{S\min})}{(n_{S\max}+n_{S\min})*2\sin\theta_S\cos\theta_S} = \frac{(n_{P\max}-n_{P\min})\cos 2\theta_P}{(n_{P\max}+n_{P\min})*2\sin\theta_P\cos\theta_P}$$

$$\frac{(n_{S\max}-n_{S\min})}{\cos\theta_S} = \frac{(n_{P\max}-n_{P\min})\cos 2\theta_P}{\cos\theta_P}$$

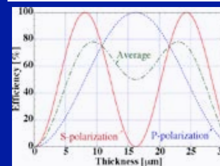

Polarized diffraction efficiencies of Dicson’s VPH grating (Polarizer) calculated by Kogelnik method. Λ= 0.646, n_L= 1.46, n_H=1.54, θ_B=48.5°.

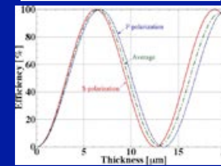

Birefringence VPH grating and calculated polarized diffraction efficiencies versus grating thick-ness *t*. Λ= 0.646 μm, n_L=1.46, n_s= 1.544, n_p = 1.60, θ_B=45°.

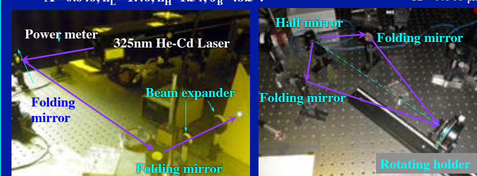

Two beam interference exposure optics for VPH grating with UV curable LC.

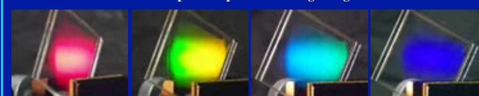

DIC TKN0100 (UV curable LC, n_o=1.5, n_e=1.55) +MJ041609, Λ~ 0.5 μm, t=1.3 μm.

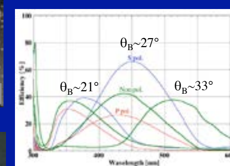

DIC ULC17A (UV curable LC, n_o=1.55, n_e=1.72)+Merck MJ041609 (normal LC, n_o=1.5, n_e=1.65), Λ~ 0.5 μm, t=10 μm.

Quasi-Bragg immersion grating

Schematic representation of quasi-Bragg immersion (QBI) grating. (Ebizuka, SPIE 6273, 2006)

QB grating with tilted mirror lattice.

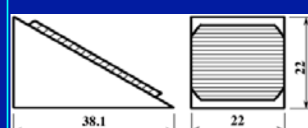

Size of QBI grating.

Block of mirror substrates stacked by fusion of gold.

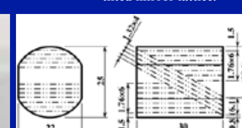

Cutting position of wire saw.

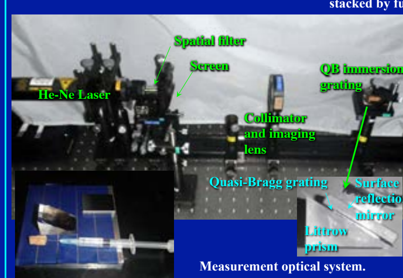

Attached by matching oil.

Measurement optical system.

Diffraction pattern (about 1,000th order) of QB grating. Beam is split up and down.

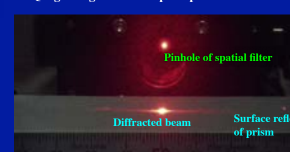

The diffracted beam is concentrated (blazed). However diffraction orders cannot separate because a point source image is larger than the interval of the diffraction orders (about 2,000th orders).

Summary

	Optimal Order	Eff. [%] (λ-λ [μm])	Status of development
Reflector facet transmission grating	2nd~	~ 80 (0.32~2.4)	Evaluations of diffraction efficiency by numerical calculations of RCWA.
Hybrid grism	2rd~	~ 70 (0.32~2.4)	Performing diamond cutting of a master grating of Ni-P alloy for MOIRCS. Replication method is under developing.
Volume binary grating	1st~	~ 80 (0.2~1000)	Performing test fabrications by using MEMS technique.
VPH grating →LC VPH grating	1st	~90 →~100 (0.32~2.4)	Installed in FOCAS, MOIRCS, Kools and WSGS2. (photopolymer) Developing new recording materials for volume hologram with liquid crystal.
Quasi-Bragg immersion grating	5th~	~ 80 (0.2~1000)	Performed test fabrications of lamination by atoms fusion bonding and lamination of embossed substrates.